Optik - International Journal for Light and Electron Optics 220 (2020) 165137

Contents lists available at ScienceDirect

Optik

journal homepage: www.elsevier.com/locate/ijleo

Influence of distance between focusing lens and sample surface on femtosecond laser-induced Cu plasma

Junfeng Shao[a], Jin Guo[a], Qiuyun Wang[b,c], Anmin Chen[b,c,*], Mingxing Jin[b,c,*]

[a] State Key Laboratory of Laser Interaction with Matter & Innovation Laboratory of Electro-Optical Countermeasures Technology, Changchun Institute of Optics, Fine Mechanics and Physics, Chinese Academy of Sciences, Changchun 130033, China

[b] Institute of Atomic and Molecular Physics, Jilin University, Changchun 130012, China

[c] Jilin Provincial Key Laboratory of Applied Atomic and Molecular Spectroscopy (Jilin University), Changchun 130012, China

ARTICLE INFO

Keywords:
Laser-Induced breakdown spectroscopy
Distance between focusing lens and sample surface
Femtosecond laser
Spectral intensity
Electron temperature

ABSTRACT

It is important to optimize emission intensity of laser-induced breakdown spectroscopy (LIBS) for improving detection sensitivity. This paper investigates the influence of the distance between focusing lens and sample surface (DBFS) on the emission line intensity and electron temperature of Cu plasma induced by femtosecond pulse laser. The results indicate that the line intensities first increase, and then drop with an increase in the DBFS. The position for obtaining highest line intensity is not the geometrical focus of the converging lens, but a short distance near the geometrical focus towards the converging lens. And the strongest emission position moves toward the converging lens as femtosecond laser energy increases. In addition, the electron temperature is calculated by using the Cu (I) lines for different DBFSs and energies. It is found that the change in the electron temperature with the DBFS is similar to that in the spectral intensity. Therefore, changing the distance is an effective way to optimize the spectral intensity in femtosecond-LIBS.

1. Introduction

Laser-induced breakdown spectroscopy (LIBS) is first proposed In 1962 [1], and now it has developed into a technology that can detect the composition and content of elements in different physical states (solid, liquid, and gas) [2–4]. The basic principle is that a beam of high-intensity laser is focused on sample surface through focusing lens to produce a high-temperature and high-bright plasma. The plasma spectrum is collected and detected by a spectrometer, and the composition and content of the elements in the sample to be measured can be obtained by analyzing the wavelength and relative intensity of the dispersed spectrum [5–10]. LIBS has many advantages including online, remote, real-time analysis, simple operation, no sample pretreatment, nearly non-destructive testing, wide range of concentration detection, simultaneous detection of multiple elements, so it is also called "green chemistry" testing technology. And it has been widely used, practical, and promising analytical technology in atomic emission spectroscopy. For these reasons, LIBS has been gradually applied in the fields of metallurgy, biomedicine, combustion, artwork identification, space research, environmental monitoring, agricultural product safety detection, harmful substance detection, archaeological exploration, industrial production, and other fields [11–14].

LIBS is expected to have higher and higher sensitivity and accuracy. Researchers begin to study how to improve spectral signal and detection sensitivity. Some methods on enhanced spectral intensity including double-pulse enhancement [15–20], discharge enhancement [21–23], spatial confinement enhancement [24–28], and magnetic confinement enhancement [29–34] are proposed. In the LIBS enhancement methods mentioned above, the use of double-pulse increases the complexity of optical devices, while the

* Corresponding authors at: Institute of Atomic and Molecular Physics, Jilin University, Changchun 130012, China.
E-mail addresses: amchen@jlu.edu.cn (A. Chen), mxjin@jlu.edu.cn (M. Jin).

https://doi.org/10.1016/j.ijleo.2020.165137
Received 8 April 2020; Accepted 12 June 2020
Available online 17 June 2020
0030-4026/

discharge, magnetic and spatial confinement enhancements require additional discharge equipment, electromagnetic field generator, and spatial confinement equipments, respectively, which increases the experimental cost. In addition, the parameters and settings of experimental equipment can affect the spectral intensity in LIBS, such as: laser characteristics (energy, pulse width) [35–40], and ambient gas pressure [41–43]. Also, the distance between focusing lens and sample surface (DBFS) can significantly change plasma spectra and plumes [44–49]. Harilal et al. reported the effect of spot diameter on generation efficiency of extreme ultraviolet in laser-ablated tin plasmas [46], finding that lens focus was not the position for optimized generation efficiency. Diego-Vallejo et al. reported the effect of the DBFS on nanosecond laser-induced copper-indium-dienamide solar cells [50], their results indicated that the focusing position could affect the signal intensity of laser-induced plasma. Wang et al. reported the effect of the DBFS on laser-ablated silicon plasma spectroscopy under standard atmospheric pressure [8], their results suggested that the emission line intensity depended on the DBFS. Zhang et al. investigated the effect of the DBFS on nanosecond-LIBS with spatial confinement [51], their results suggested that the spectral emission signal could be optimized by changing lens focusing distance. Singh et al. discussed the influence of focusing lens position on laser-ablated copper plasma with magnetic confinement under atmospheric pressure [31]. Chen et al. studied the effect of the DBFS on laser-ablated zinc plasma [52], their results indicated that the DBFS would affect the area and depth of the ablated sample, and a stronger spectral emission signal could be obtained by selecting a appropriate lens focusing distance.

In the examples above, nanosecond laser is used as the laser excitation source, but one of its disadvantages is plasma shielding effect due to the interaction between plasma and nanosecond laser [53]. The plasma shielding greatly reduces the energy absorbed by the target. However, femtosecond pulse laser can avoid this problem due to very short pulse width. Compared with nanosecond laser, femtosecond laser has a very high peak power [54,55]. The advantage enables the femtosecond laser to inject enough energy into ablated target in a very short time, and the plasma forms rapidly and does not interact with the laser to cause energy loss. And, the femtosecond laser energy is stable and has strong repeatability, so it is easy to repeat or reproduce experimental process in practical operation [56]. At the same time, femtosecond laser can ionize the target quickly in a very short time, the heat affected area is small, the molecular structure is not damaged [57]. And then, femtosecond pulse laser is widely used to study LIBS. As discussed above, the DBFS can influence the spectral intensity of nanosecond-LIBS, and is also directly related to the plasma shielding effect [8,48,58,59], while there is almost no shielding effect in femtosecond-LIBS. The influence of the DBFS on emission line intensity of femtosecond-LIBS will be different from nanosecond-LIBS. Therefore, it is necessary to discuss the influence of the DBFS on the emission line of femtosecond-LIBS.

In this study, the influence of the DBFS on spectral emission characteristics of femtosecond laser-ablated Cu plasmas was investigated in air. The change in the line intensity with the DBFS for different laser energies was discussed. And, electron temperature was calculated using measured Cu (I) lines, the changes in the electron temperature and line intensity with the DBFS showed a similar trend.

2. Experimental setup

The Experimental setup of femtosecond-LIBS is illustrated in Fig. 1. A ultrafast Ti:sapphire regenerative amplifier laser system (Coherence, Libra) was used as excitation source. The laser wavelength was 800 nm, and the laser pulse width was 50 fs. Both a half wave plate (800 nm) and a Glan laser polarizer attenuated laser energy to a desired value. A focusing lens (focal length = 10 cm) converged laser beam on Cu sample surface, forming Cu plasma. The Cu sample was attached on a compute-controlled 3D stage (PT3/MZ8, Thorlabs) to ensure that the laser hit new sample surface for each laser shot. In order to change the DBFS, the focusing lens was attached on a computer controlled linear translation stage (zolix). A plane-convex lens (focal length = 75 mm, diameter = 50 mm) collected optical emission, and focused the collected optical emission into a fiber, and the fiber was coupled with a spectrometer (Princeton-instruments, SP500i, PIActon, 1200 lines/mm). The dispersed light by the spectrometer was detected using an ICCD (Princeton-instruments, PIMAX4, 1024i). The synchronization and delay generator (SDG) of the laser system triggered the ICCD detector to synchronize the time between laser signal and plasma signal. The laser system used single laser shot mode to perform spectral measurement, and 50 laser shots was averaged to reduce the spectral fluctuation. The experiment was carried out under standard atmospheric pressure, 22 °C room temperature, and 40 % relative humidity.

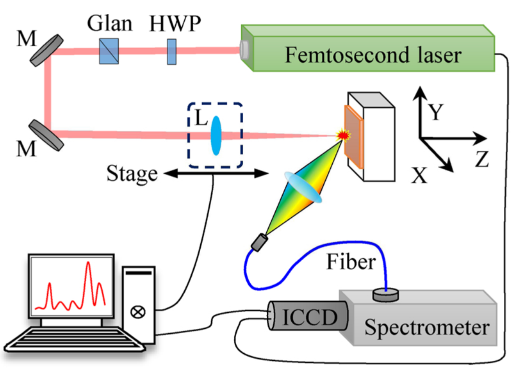

Fig. 1. Experimental setup of femtosecond-LIBS of Cu sample (M is the mirror; L is the lens; HWP is the half-wave plate; Glan is the Glan laser polarizer; and ICCD is the intensified CCD).

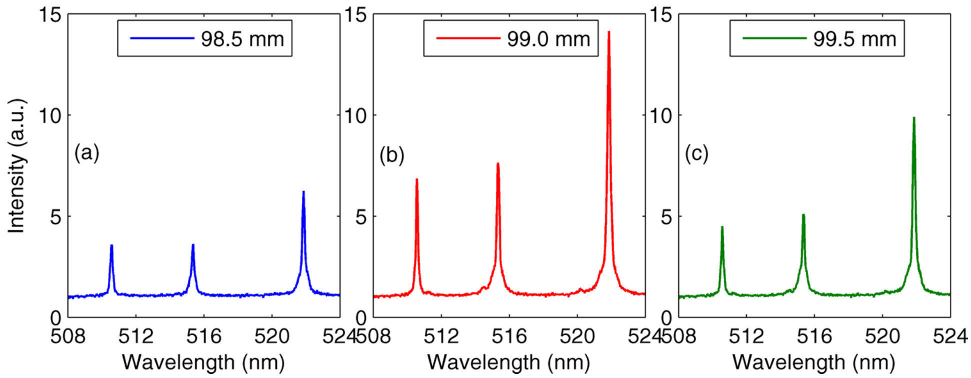

Fig. 2. Spectra of femtosecond-LIBS of Cu target for three DBFSs (98.5, 99.0, and 99.5 mm) at 1.0 mJ laser energy.

3. Results and discussion

To compare the line intensity of femtosecond-LIBS for different DBFSs, Fig. 2 presents the spectra of femtosecond-LIBS of Cu target for three DBFSs (98.5, 99.0, and 99.5 mm) at 1.0 mJ laser energy. Three transition lines can be observed, which are located at Cu (I) 510.55 nm, Cu (I) 515.32 nm, and Cu (I) 521.82 nm, respectively. As shown in the figure, the strongest emission among the three spectral lines is at the distance of 99.0 mm, and the lowest one is at the distance of 98.5 mm. The phenomenon indicates that a stronger spectral emission can be obtained by selecting an appropriate DBFS.

In order to further understand the influence of the DBFS on the line intensity of femtosecond-LIBS, Fig. 3(a) shows the distribution of optical emission with the DBFS and wavelength on femtosecond-LIBS of Cu target. The laser energy is 1.0 mJ. Based on the figure, the evolution of peak emission of Cu (I) 521.82 nm with the DBFS is displayed in Fig. 3(b). It can be seen from Fig. 3(b) that the emission line of femtosecond-LIBS depends on the DBFS. The line intensity increases monotonously as the DBFS increases; at 99.2 mm, the line reaches highest emission intensity; continue to increase the DBFS, the line intensity begins to decrease. Since the laser energy is constant in the process of changing the DBFS, the change in the DBFS is equivalent to that in the laser fluence, that is to say, as the focusing lens moves, it is equivalent to change the laser spot diameter on the sample surface [45,60,61]. In this experiment, when the distance changes from 98.0 mm to 99.2 mm, the spot diameter decreases, while the laser fluence increases, resulting in an increase in the peak of Cu (I) line; as the DBFS changes 99.2 mm–100.5 mm, the spot diameter increases, while the laser fluence decreases, leading to a reduction in the peak emission of Cu (I) line; at the DBFS of 99.2 mm, the peak intensity of Cu (I) line is highest, which is the best position of the focusing lens.

In addition, geometrical focus of the converging lens used is not the strongest emission position but a short distance near the geometrical focus towards the converging lens. When ultrashort pulse ablates the target in air, the nonlinear effect of ultrashort pulse can change laser focusing position of converging lens. The ultrashort pulse can change the refractive index of air under strong laser field [62,63]. The relationship between refractive index (n) and incident laser intensity is as follows [63]:

$$n = n_0 + n_2 I \tag{1}$$

where, I, n_0, and n_2 represent the laser intensity, the linear refractivity, and the nonlinear refractive index coefficient, respectively. Femtosecond laser intensity is not evenly distributed on the cross section, the uneven distribution can cause the change of phase velocity during femtosecond laser propagation. The phase velocity $v_{phase} = c_0 / n$, c_0 is the speed of light in vacuum. In current experiment, due to the Gaussian distribution on the cross section, the center intensity is higher, so the refractive index in the laser center is higher compared with that around the laser center, leading to the higher phase velocity in the laser center is lower than that

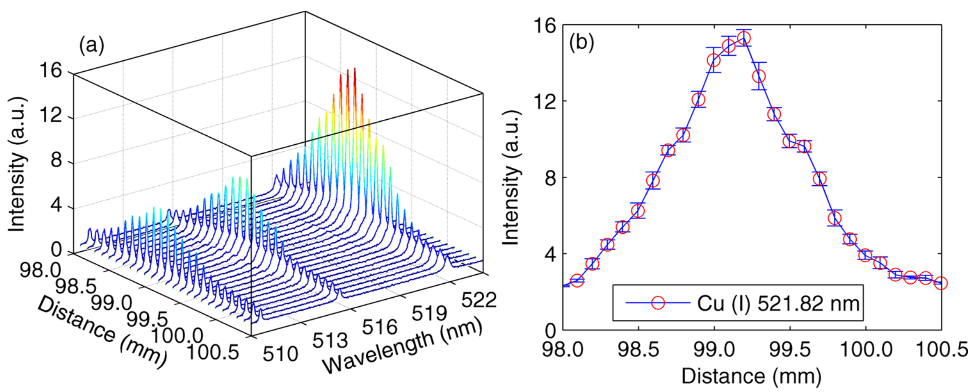

Fig. 3. (a) Distribution of optical emission with DBFS and wavelength; (b) evolution of peak intensity of Cu (I) 521.82 nm with DBFS.

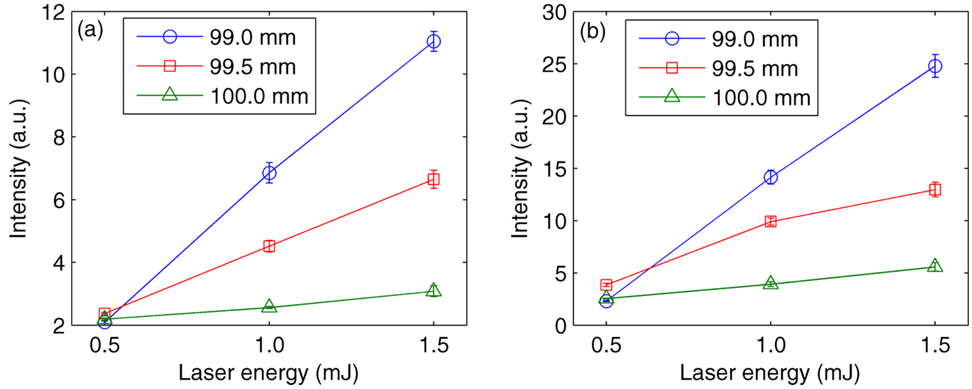

Fig. 4. Evolution of peak intensities of Cu (I) 510.55 nm (a) and 521.82 nm (b) lines as functions of laser energy for different DBFSs (99.0, 99.5, and 100.0 mm).

around the laser center. The v_{phase} will be changed into a concave wave, which makes femtosecond laser converge, generating self-focusing effect of femtosecond laser [43,64–66]. As a result, the actual focus of femtosecond laser beam in the experiment moves toward the converging lens, leading to the movement of the position for strongest spectral emission. In nanosecond-LIBS, the change in the line intensity with the DBFS has a similar trend with femtosecond-LIBS. But, the mechanism of the change differs from femtosecond-LIBS. The mechanism of the change is based on plasma shielding effect of nanosecond laser [53]. Nanosecond laser has longer pulse duration compared with femtosecond laser. When nanosecond laser irradiates the sample surface, a high-temperature and high-density plasma is produced by the pulse leading edge. Subsequently, the energy of the pulse trailing edge will be absorbed by the produced plasma, and expands rapidly, preventing the laser from reaching the sample surface.

Moreover, femtosecond laser energy is also an important factor affecting the intensity of Cu (I) lines. Fig. 4 illustrates the evolution of emission peaks of Cu (I) 510.55 nm and 521.82 nm lines with laser energy for three DBFSs. The DBFSs are 99.0, 99.5, and 100.0 mm, respectively. The emission intensities of Cu (I) 510.55 nm and 521.82 nm lines show same trend as the laser energy increases. For the distance of 99.0 mm, the increase in the peak is the most obvious. However, the change in the peak intensity at the distance of 100.0 mm is very small. The result indicates that, as the laser energy increases, the DBFS has a great influence on the spectral intensity. Next, the changes in the spectral intensity with the DBFS under different laser energies are studied in detail.

Fig. 5 presents the evolution of peak intensities of Cu (I) 510.55 and 521.82 nm lines as functions of the DBFS for different laser energies. The laser energies are 0.5, 1.0 and 1.5 mJ, respectively. The spectral peak intensity with higher laser energy is than that with lower laser energy, and the position for obtaining highest spectral intensity moves toward the converging lens when laser energy increases. For the increase of the spectra line intensity of femtosecond-LIBS, the excited atom number density and transition probability are directly proportional to optical emission, if the transition probability remains unchanged, the excited atom number density is positively related to optical emission [67]. Increasing the laser energy can increase the ablation mass of Cu sample and generate stronger Cu plasma, which will increase the number density of excited atoms and increase the spectral intensity of Cu plasma. For the movement of the position for obtaining highest spectral intensity, the physical mechanism can be explained by se following theory. The change in the position for obtaining highest spectra is related to the propagation length (L_c) of femtosecond laser in air [64,65]. L_c can be described by the following formula [64,68]:

$$L_c = \frac{0.367k_0r_0^2}{\sqrt{((P_{in}/P_{cr})^{1/2} - 0.852)^2 - 0.0219}} \tag{2}$$

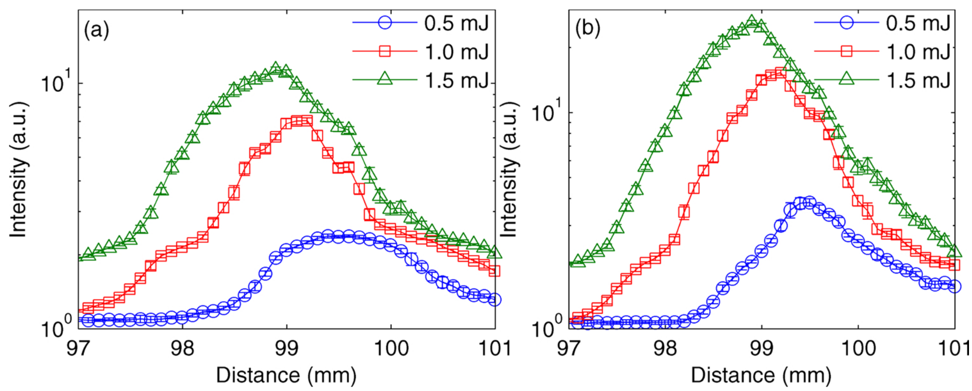

Fig. 5. Evolution of peak intensities of Cu (I) 510.55 (a) and 521.82 (b) lines as functions of DBFS for different laser energies (0.5, 1.0 and 1.5 mJ).

Table 1
Spectral parameters of three Cu (I) lines.

Line	Wavelength λ_{mn} (nm)	Transition	g_m(Upper-level degeneracy)× A_{mn}(Transition probability)	Upper-level energy E_m (eV)
Cu(I)	510.55	$3d^{10}4p(^2P_{3/2}) - 3d^94s^2(^2D_{5/2})$	8.0×10^6	3.82
Cu(I)	515.32	$3d^{10}4d(^2D_{3/2}) - 3d^{10}4p(^2P_{1/2})$	2.4×10^8	6.19
Cu(I)	521.82	$3d^{10}4d(^2D_{5/2}) - 3d^{10}4p(^2P_{3/2})$	4.5×10^8	6.19

P_{in}, $P_{cr} = 3.77\lambda_0^2/8\pi n_0 n_2$ r_0 $k_0 = 2\pi/\lambda_0$ and λ_0 represent the initial laser power, the critical power, the beam radius, the wave number, and the laser wavelength, respectively. So, L_c is positively related to P_{in}. For converging laser, the converged distance (L_{cf}) can be expressed by the focal length transformation formula [43,65]:

$$\frac{1}{L_{cf}} = \frac{1}{L_c} + \frac{1}{f} \tag{3}$$

f is the focal distance of lens. So, L_{cf} is positively related to P_{in}. Therefore, P_{in} increases with the increase of laser energy, resulting in an increase in the L_{cf}. So, the positions for obtaining strongest spectra move toward the converging lens as laser energy increases.

Finally, it is also important to study the influence of the DBFS on electron temperature of plasma. When obtaining the electron temperature, firstly, it is assumed that the laser-induced Cu plasma satisfies the conditions of optical thin film and local thermal equilibrium (LTE); secondly, the relative intensities of several spectral lines are measured. In current experiment, we obtained the Cu (I) 510.55 nm, Cu (I) 515.32 nm, and Cu (I) 521.82 nm, the three lines can satisfy the needs of calculating the electron temperature. The slope method (or Boltzmann plot) is commonly used to calculate the electron temperature, and the formula is as follows [59,69,70]:

$$In\frac{\lambda_{mn}}{g_m A_{mn}} = -\frac{E_m}{k_B T} + C \tag{4}$$

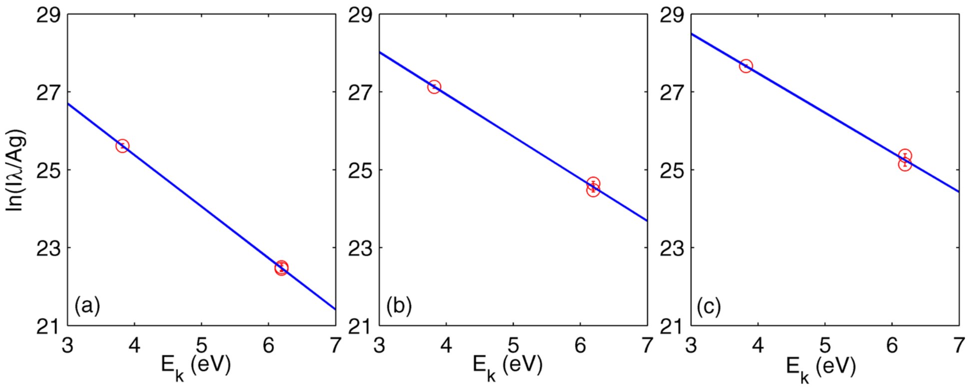

Fig. 6. Typical Boltzmann plot of femtosecond laser-induced plasma spectroscopy at 99.0 mm distance for three laser energies. The laser energies are 0.5 (a), 1.0 (b), and 1.5 (c) mJ.

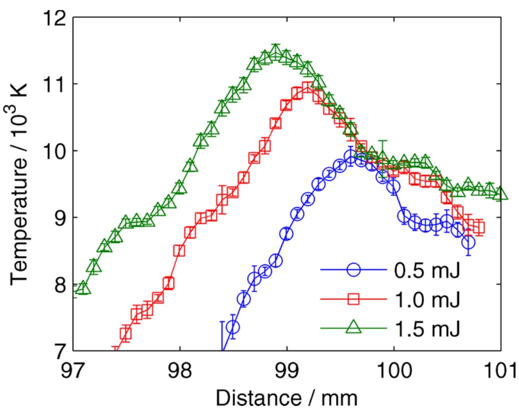

Fig. 7. Evolution of electron temperatures with DBFS for three laser energies (0.5, 1.0, and 1.5 mJ).

where, m and n represent the upper and lower levels, I_{mn} is the line intensity, k_B is the Boltzmann constant, g_m is the statistical weight at upper level, A_{mn} is the transition probability, E_m is the upper level energy, λ_{mn} is the emission line wavelength, C is the constant, and T is the electron temperature. All of the spectral parameters g_m, A_{mn}, and E_m are listed in Table 1. Fig. 6 presents the typical Boltzmann plot of Cu plasma spectra for three laser energies at the DBFS of 99.0 mm. The laser energies are 0.5, 1.0, and 1.5 mJ. Fig. 7 presents the evolution of electron temperatures with the DBFS for the three laser energies. It is observed that the change in the electron temperature with the DBFS is similar to that in the emission intensity with the DBFS (see Fig. 5), that is, the electron temperature first increases and then decreases as the DBFS increases, and the position for obtaining highest electron temperature also moves toward the focusing lens. As mentioned above, stronger laser focusing produces higher temperature and density plasma, the plasma with higher temperature can emit stronger optical emission. The change in the electron temperature with the DBFS can better understand the stronger spectral emission optimized by selecting a suitable DBFS.

4. Conclusions

The spectral emission intensity of LIBS can be optimized by changing the DBFS. The influence of the DBFS on the spectra of femtosecond laser-induced Cu plasmas in air was investigated by measuring the Cu (I) lines at 510.55, 515.32, and 521.82 nm. The Cu (I) line intensities first increased and then decreased with an increase in the DBFS. As the laser energy increased, the position for obtaining highest line intensity moved toward the converging lens due to the self-focusing effect of femtosecond laser. Also, the electron temperature was calculated, finding that the change in the electron temperature with the DBFS and laser energy were similar to that in the spectral intensity. The electron temperature provided better understanding for the influence of the DBFS on the spectral line intensity of femtosecond-LIBS. Therefore, the spectral line intensity of femtosecond-LIBS can be optimized by changing the DBFS. Finally, we hope that this work will be helpful to understand the influence of the DBFS on femtosecond-LIBS.

Declaration of Competing Interest

The authors declare that they have no known competing financial interests or personal relationships that could have appeared to influence the work reported in this paper.

Acknowledgements

We acknowledge the support by National Natural Science Foundation of China (Nos. 11674128, 11674124 and 11974138), the Jilin Province Scientific and Technological Development Program, China (Grant No. 20170101063JC), and the Scientific and Technological Research Project of the Education Department of Jilin Province, China (No. JJKH20200937KJ).

References

[1] F. Brech, L. Cross, Optical microemission stimulated by a ruby laser, Appl. Spectrosc. 16 (1962) 59–64.
[2] P. Fichet, P. Mauchien, J.F. Wagner, C. Moulin, Quantitative elemental determination in water and oil by laser induced breakdown spectroscopy, Anal. Chim. Acta 429 (2001) 269–278.
[3] J. Gruber, J. Heitz, H. Strasser, D. Bauerle, N. Ramaseder, Rapid in-situ analysis of liquid steel by laser-induced breakdown spectroscopy, Spectrochim. Acta Part B At. Spectrosc. 56 (2001) 685–693.
[4] A. Chen, Y. Jiang, T. Wang, J. Shao, M. Jin, Comparison of plasma temperature and electron density on nanosecond laser ablation of Cu and nano-Cu, Phys. Plasmas 22 (2015) 033301.
[5] Z. Wang, T.B. Yuan, Z.Y. Hou, W.D. Zhou, J.D. Lu, H.B. Ding, X.Y. Zeng, Laser-induced breakdown spectroscopy in China, Front. Phys. 9 (2014) 419–438.
[6] Y. Fu, Z. Hou, Y. Deguchi, Z. Wang, From big to strong: growth of the Asian laser-induced breakdown spectroscopy community, Plasma Sci. Technol. 21 (2019) 030101.
[7] D. Zhang, A. Chen, Q. Wang, Y. Wang, S. Li, Y. Jiang, M. Jin, Effect of lens focusing distance on laser-induced silicon plasmas at different sample temperatures, Plasma Sci. Technol. 21 (2019) 034009.
[8] Y. Wang, A. Chen, S. Li, D. Ke, X. Wang, D. Zhang, Y. Jiang, M. Jin, Influence of distance between sample surface and focal point on spectral intensity of nanosecond laser-induced silicon plasma in air, AIP Adv. 7 (2017) 095204.
[9] J. Guo, J. Shao, T. Wang, C. Zheng, A. Chen, M. Jin, Optimization of distances between the target surface and focal point on spatially confined laser-induced breakdown spectroscopy with a cylindrical cavity, J. Anal. At. Spectrom. 32 (2017) 367–372.
[10] Z. Wang, F. Dong, W. Zhou, A rising force for the world-wide development of laser-induced breakdown spectroscopy, Plasma Sci. Technol. 17 (2015) 617.
[11] A.K. Knight, N.L. Scherbarth, D.A. Cremers, M.J. Ferris, Characterization of laser-induced breakdown spectroscopy (LIBS) for application to space exploration, Appl. Spectrosc. 54 (2000) 331–340.
[12] D. Rusak, B. Castle, B. Smith, J. Winefordner, Fundamentals and applications of laser-induced breakdown spectroscopy, Crit. Rev. Anal. Chem. 27 (1997) 257–290.
[13] A.F.M.Y. Haider, Z.H. Khan, Determination of Ca content of coral skeleton by analyte additive method using the LIBS technique, Opt. Laser Technol. 44 (2012) 1654–1659.
[14] S.S. Harilal, B.E. Brumfield, N.L. Lahaye, K.C. Hartig, M.C. Phillips, Optical spectroscopy of laser-produced plasmas for standoff isotopic analysis, Appl. Phys. Rev. 5 (2018) 021301.
[15] C. Song, X. Gao, Y. Shao, Pre-ablation laser parameter effects on the spectral enhancement of 1064nm/1064nm dual-pulse laser induced breakdown spectroscopy, Optik 127 (2016) 3979–3983.
[16] A. Hussain, X. Gao, Z. Hao, J. Lin, Combined effects of double pulses and magnetic field on emission enhancement of laser-induced breakdown spectroscopy from aluminum plasma, Optik 127 (2016) 10024–10030.
[17] Y. Wang, A. Chen, Q. Wang, D. Zhang, L. Sui, S. Li, Y. Jiang, M. Jin, Enhancement of optical emission generated from femtosecond double-pulse laser-induced glass plasma at different sample temperatures in air, Plasma Sci. Technol. 21 (2019) 034013.
[18] D. Zhang, A. Chen, X. Wang, S. Li, Y. Wang, L. Sui, Y. Jiang, M. Jin, Enhancement mechanism of femtosecond double-pulse laser-induced Cu plasma spectroscopy, Opt. Laser Technol. 96 (2017) 117–122.

[19] P.K. Diwakar, S.S. Harilal, J.R. Freeman, A. Hassanein, Role of laser pre-pulse wavelength and inter-pulse delay on signal enhancement in collinear double-pulse laser-induced breakdown spectroscopy, Spectrochim. Acta Part B At. Spectrosc. 87 (2013) 65–73.
[20] Y. Wang, A. Chen, S. Li, L. Sui, D. Liu, S. Li, H. Li, Y. Jiang, M. Jin, Re-heating effect on the enhancement of plasma emission generated from Fe under femtosecond double-pulse laser irradiation, Plasma Sci. Technol. 18 (2016) 1192–1197.
[21] Y. Wang, Y. Jiang, X. He, Y. Chen, R. Li, Triggered parallel discharge in laser-ablation spark-induced breakdown spectroscopy and studies on its analytical performance for aluminum and brass samples, Spectrochim. Acta Part B At. Spectrosc. 150 (2018) 9–17.
[22] W. Zhou, X. Su, H. Qian, K. Li, X. Li, Y. Yu, Z. Ren, Discharge character and optical emission in a laser ablation nanosecond discharge enhanced silicon plasma, J. Anal. At. Spectrom. 28 (2013) 702–710.
[23] Q. Wang, A. Chen, W. Xu, D. Zhang, Y. Wang, S. Li, Y. Jiang, M. Jin, Time-resolved spectroscopy of femtosecond laser-induced Cu plasma with spark discharge, Plasma Sci. Technol. 21 (2019) 065504.
[24] H.L. Yin, Z.Y. Hou, T.B. Yuan, Z. Wang, W.D. Ni, Z. Li, Application of spatial confinement for gas analysis using laser-induced breakdown spectroscopy to improve signal stability, J. Anal. At. Spectrom. 30 (2015) 922–928.
[25] C.M. Li, L.B. Guo, X.N. He, Z.Q. Hao, X.Y. Li, M. Shen, X.Y. Zeng, Y.F. Lu, Element dependence of enhancement in optics emission from laser-induced plasma under spatial confinement, J. Anal. At. Spectrom. 29 (2014) 638–643.
[26] W. Xu, A. Chen, Q. Wang, D. Zhang, S. Li, Y. Jiang, X. Gao, M. Jin, Characteristics of laser-induced aluminum plasma plumes after increasing sample temperature and spatial confinement, J. Anal. At. Spectrom. 34 (2019) 2288–2294.
[27] Q. Wang, A. Chen, D. Zhang, Y. Wang, L. Sui, S. Li, Y. Jiang, M. Jin, The role of cavity shape on spatially confined laser-induced breakdown spectroscopy, Phys. Plasmas 25 (2018) 073301.
[28] J. Shao, J. Guo, Q. Wang, A. Chen, M. Jin, Spatial confinement effect on CN emission from nanosecond laser-induced PMMA plasma in air, Optik 207 (2020) 164448.
[29] Y. Lu, Y.S. Zhou, W. Qiu, X. Huang, L. Liu, L. Jiang, J.F. Silvain, Y.F. Lu, Magnetic field enhancement for femtosecond-laser-ablation mass spectrometry in ambient environments, J. Anal. At. Spectrom. 30 (2015) 2303–2306.
[30] P.K. Pandey, R.K. Thareja, Rotating copper plasmoid in external magnetic field, Phys. Plasmas 20 (2013) 022117.
[31] K.S. Singh, A.K. Sharma, Spatially resolved behavior of laser-produced copper plasma along expansion direction in the presence of static uniform magnetic field, Phys. Plasmas 23 (2016) 122104.
[32] S.S. Harilal, B.O. Shay, M.S. Tillack, C.V. Bindhu, F. Najmabadi, Fast photography of a laser generated plasma expanding across a transverse magnetic field, Ieee Trans. Plasma Sci. 33 (2005) 474–475.
[33] A. Hussain, M. Tanveer, G. Farid, M.B. Hussain, M. Azam, W. Khan, Combined effects of magnetic field and ambient gas condition in the enhancement of laser-induced breakdown spectroscopy signal, Optik 172 (2018) 1012–1018.
[34] S. Waheed, S. Bashir, A. Dawood, S. Anjum, M. Akram, A. Hayat, S. Amin, A. Zaheer, Effect of magnetic field on laser induced breakdown spectroscopy of zirconium dioxide (ZrO2) plasma, Optik 140 (2017) 536–544.
[35] S.S. Harilal, T. Sizyuk, A. Hassanein, D. Campos, P. Hough, V. Sizyuk, The effect of excitation wavelength on dynamics of laser-produced tin plasma, J. Appl. Phys. 109 (2011) 056403.
[36] B.L. Drogoff, J. Margot, F. Vidal, S. Laville, M. Chaker, M. Sabsabi, T.W. Johnston, O. Barthélemy, Influence of the laser pulse duration on laser-produced plasma properties, Plasma Sources Sci. Technol. 13 (2004) 223.
[37] J. Wu, W. Wei, X. Li, S. Jia, A. Qiu, Infrared nanosecond laser-metal ablation in atmosphere: initial plasma during laser pulse and further expansion, Appl. Phys. Lett. 102 (2013) 101501.
[38] A.M. Chen, Y.F. Jiang, H. Liu, M.X. Jin, D.J. Ding, Plume splitting and rebounding in a high-intensity CO2 laser induced air plasma, Phys. Plasmas 19 (2012) 073302.
[39] Y. Wang, A. Chen, L. Sui, S. Li, D. Liu, X. Wang, Y. Jiang, X. Huang, M. Jin, Persistence of atomic spectral line on laser-induced Cu plasma with spatial confinement, Phys. Plasmas 23 (2016) 113105.
[40] A. Chen, S. Li, S. Li, Y. Jiang, J. Shao, T. Wang, X. Huang, M. Jin, D. Ding, Optimally enhanced optical emission in laser-induced air plasma by femtosecond double-pulse, Phys. Plasmas 20 (2013) 103110.
[41] M. Kuzuya, O. Mikami, Effect of argon atmosphere on self-absorption of a spectral line in laser microprobe analysis, J. Appl. Phys. 29 (1990) 1568–1569.
[42] W. Sdorra, K. Niemax, Basic investigations for laser microanalysis: III. Application of different buffer gases for laser-produced sample plumes, Microchim. Ichnoanal. Acta 107 (1992) 319–327.
[43] Q.X. Wang, A.M. Chen, S.Y. Li, H.X. Qi, Y. Qi, Z. Hu, M.X. Jin, Influence of ambient pressure on the ablation hole in femtosecond laser drilling Cu, Appl. Opt. 54 (2015) 8235–8240.
[44] S.S. Harilal, P.K. Diwakar, M.P. Polek, M.C. Phillips, Morphological changes in ultrafast laser ablation plumes with varying spot size, Opt. Express 23 (2015) 15608–15615.
[45] X. Li, W. Wei, J. Wu, S. Jia, A. Qiu, The Influence of spot size on the expansion dynamics of nanosecond-laser-produced copper plasmas in atmosphere, J. Appl. Phys. 113 (2013) 243304.
[46] S.S. Harilal, R.W. Coons, P. Hough, A. Hassanein, Influence of spot size on extreme ultraviolet efficiency of laser-produced Sn plasmas, Appl. Phys. Lett. 95 (2009) 1549.
[47] D. Zhang, A. Chen, X. Wang, Y. Wang, L. Sui, D. Ke, S. Li, Y. Jiang, M. Jin, Influence of the distance between target surface and focal point on the expansion dynamics of a laser-induced silicon plasma with spatial confinement, Spectrochim. Acta Part B At. Spectrosc. 143 (2018) 71–77.
[48] K. Guo, A. Chen, X. Gao, Influence of distance between target surface and focal point on CN emission of nanosecond laser-induced PMMA plasma in air, Optik (2019), https://doi.org/10.1016/j.ijleo.2019.164067.
[49] D. Zhang, A. Chen, Q. Wang, W. Xu, Y. Wang, S. Li, Y. Jiang, M. Jin, Influence of distance between sample surface and focal point on the expansion dynamics of laser-induced silicon plasma under different sample temperatures in air, Optik 202 (2020) 163511.
[50] D. Diego-Vallejo, D. Ashkenasi, A. Lemke, H.J. Eichler, Selective ablation of Copper-Indium-Diselenide solar cells monitored by laser-induced breakdown spectroscopy and classification methods, Spectrochim. Acta Part B At. Spectrosc. 87 (2013) 92–99.
[51] Z. Jiang, S. Junfeng, W. Tingfeng, G. Jin, D. Zhang, Effect of distances between lens and sample surface on laser-induced breakdown spectroscopy with spatial confinement, Plasma Sci. Technol. 20 (2018) 085503.
[52] M. Chen, Y. Liu, X. Liu, M. Zhao, Role of lens to sample distance during laser-induced damage in zinc targets, Laser Phys. Lett. 9 (2012) 730.
[53] A. Semerok, C. Dutouquet, Ultrashort double pulse laser ablation of metals, Thin Solid Films 453-54 (2004) 501–505.
[54] T. Wang, J. Guo, J. Shao, D. Wang, A. Chen, M. Jin, Ultrafast thermionic emission from metal irradiated using a femtosecond laser and an electric field in combination, Phys. Plasmas 22 (2015) 033106.
[55] A. Chen, L. Sui, Y. Shi, Y. Jiang, D. Yang, H. Liu, M. Jin, D. Ding, Ultrafast investigation of electron dynamics in the gold-coated two-layer metal films, Thin Solid Films 529 (2013) 209–216.
[56] Y. Wang, A. Chen, S. Li, L. Sui, D. Liu, D. Tian, Y. Jiang, M. Jin, Enhancement of laser-induced Fe plasma spectroscopy with dual-wavelength femtosecond double-pulse, J. Anal. At. Spectrom. 31 (2016) 497–505.
[57] M. Baudelet, L. Guyon, J. Yu, J.-P. Wolf, T. Amodeo, E. Fréjafon, P. Laloi, Femtosecond time-resolved laser-induced breakdown spectroscopy for detection and identification of bacteria: a comparison to the nanosecond regime, J. Appl. Phys. 99 (2006) 084701.
[58] D. Diego-Vallejo, D. Ashkenasi, H.J. Eichler, Monitoring of focus position during laser processing based on plasma emission, Phys. Procedia 41 (2013) 911–918.
[59] Y. Wang, A. Chen, Q. Wang, L. Sui, D. Ke, S. Cao, S. Li, Y. Jiang, M. Jin, Influence of distance between focusing lens and target surface on laser-induced Cu plasma temperature, Phys. Plasmas 25 (2018) 033302.
[60] S.S. Harilal, R.W. Coons, P. Hough, A. Hassanein, Influence of spot size on extreme ultraviolet efficiency of laser-produced Sn plasmas, Appl. Phys. Lett. 95 (2009) 221501.

[61] Y. Wang, A. Chen, S. Li, D. Ke, X. Wang, Influence of distance between sample surface and focal point on spectral intensity of nanosecond laser-induced silicon plasma in air, AIP Adv. 7 (2017) 095204.
[62] H. Schillinger, R. Sauerbrey, Electrical conductivity of long plasma channels in air generated by self-guided femtosecond laser pulses, Appl. Phys. B 68 (1999) 753–756.
[63] S.L. Chin, Femtosecond Laser Filamentation, Springer, 2010.
[64] A. Couairon, M. Franco, G. Méchain, T. Olivier, B. Prade, A. Mysyrowicz, Femtosecond filamentation in air at low pressures: part I: theory and numerical simulations, Opt. Commun. 259 (2006) 265–273.
[65] A. Couairon, A. Mysyrowicz, Femtosecond filamentation in transparent media, Phys. Rep. 441 (2007) 47–189.
[66] H. Qi, S. Li, Y. Qi, A. Chen, Z. Hu, X. Huang, M. Jin, D. Ding, Effect of sample position on collinear femtosecond double-pulse laser-induced breakdown spectroscopy of silicon in air, J. Anal. At. Spectrom. 29 (2014) 1105–1111.
[67] X. Li, Z. Yang, J. Wu, W. Wei, Y. Qiu, S. Jia, A. Qiu, Spatial confinement in laser-induced breakdown spectroscopy, J. Phys. D Appl. Phys. 50 (2017) 015203.
[68] S.-Y. Li, F.-M. Guo, Y. Song, A.-M. Chen, Y.-J. Yang, M.-X. Jin, Influence of group-velocity-dispersion effects on the propagation of femtosecond laser pulses in air at different pressures, Phys. Rev. A 89 (2014) 023809.
[69] C.A. Bye, A. Scheeline, Saha-Boltzmann statistics for determination of electron temperature and density in spark discharges using an Echelle/CCD system, Appl. Spectrosc. 47 (1993) 2022–2030.
[70] D.-P. Yang, S.-Y. Li, Y.-F. Jiang, A.-M. Chen, M.-X. Jin, Temperature and electron density in femtosecond filament-induced Cu plasma, Acta Phys. Sin. 66 (2017) 115201.